Romanian Reports in Physics, Vol. 60, No. 3, P. 701–711, 2008

Dedicated to Prof. Ioan-Iovitz Popescu's 75th Anniversary

IRON RICH-RARE-EARTH COMPOUNDS: BASIC AND PERMANENT MAGNETIC PROPERTIES

E. BURZO

Faculty of Physics, "Babes-Bolyai" University, 400084, Cluj-Napoca, Romania

Received Feburary 5, 2008

Abstract. Band structure calculations were performed on $R_2Fe_{14}B$ and R_2Fe_{17} type compounds, where R is a rare–earth. The exchange interactions in these systems were analysed. The iron moments at various lattice sites as well as R5d band polarizations are linearly dependent on De Gennes factor. The contributions of intra atomic and short range exchange interactions to R5d band polarizations were analysed. Then, the magnetic properties and magnetocaloric effects in Nd–Fe–Si–B permanent magnets were discussed,. The volume variation of Curie temperatures, T_C, in carbonated nanocrystalline 1/9 and 2/17 systems are linearly dependent on T_C values, showing a rather high degree of iron moments localization. The effective exchange interactions in 1/9 phases are more sensitive to volume variations than in case of 2/17 compounds.

Key word: band structure, rare earth compunds, magnetic properties, iron moments.

1. INTRODUCTION

The rare-earth(R)–transition metal(M) (M = Co,Fe) compounds are of great interest both from scientific point of view as well as for their technical applications, particularly as permanents magnets. The rare-earth cobalt permanent magnets are based on $SmCo_5$ and Sm_2Co_{17} type compounds. These have high Curie temperatures, mainly determined by the contribution of cobalt sublattice to the exchange interactions. Both cobalt and samarium are expensive. Thus, the researches were directed on iron–based intermetallic compounds as possible candidates for permanent magnet manufacturing.

The studies performed on iron-rich intermetallic compounds evidenced rather low Curie temperatures, T_C. For R_2Fe_{17} system, the highest value, T_C = 477 K, was evidenced for R = Gd [1]. Somewhat higher Curie temperatures, around 600 K, were found in $R_2Fe_{14}B$ system [2]. The above mentioned values are about half of the T_C value of pure iron, although the iron content in the above compounds is 90 at % and 82 at %, respectively. In both systems, the mean iron moments are

close to that of pure iron, $M_{fe} = 2.22\ \mu_B$. Due to low T_C values and planar anisotropies, the R_2Fe_{17} compounds have been considered as being not useful for technical applications, such as permanent magnets. In spite of relatively low Curie points, the R–Fe–B magnets, based on $R_2Fe_{14}B$ phases, have excellent properties at room temperature. Researches are directed to improve their performances at higher temperatures. This is an important request for technical uses, since from economical point of view the iron-based magnets have advantage over the cobalt–based ones, due to more abundance of the raw materials and consequently lower cost.

The exchange interactions in R–M and R–M–B compounds, between rare-earths and transition metals can be described by the 4f–5d–3d model [3]. In this model, the 4f moments induce a positive polarization on their 5d band through the ordinary intra-atomic 4f–5d or 4f–6s exchange with subsequent direct 5d–nd exchange interactions with other nd shells of neighbouring atoms. There are also short-range exchange interactions of 3d–3d type between the transition metal atoms.

The R_2Fe_{17} and $R_2Fe_{14}B$ compounds have relative complex crystalline structures in which both the R and Fe atoms occupy different sites. Thus, in both $P6_3/mmc$ and $R\bar{3}m$ type structures, in which crystallize R_2Fe_{17} compounds, iron is distributed in four lattice sites and R atoms in two or one, respectively. The tetragonal $P4_2/mmm$ lattice of $R_2Fe_{14}B$ compounds has six different iron sites, two for R sites and one for B. For a given iron lattice site, the distances between iron atoms, d_{FeFe}, cover a large range of values. The interactions between iron atoms situated at distances $d_{FeFe} < 2.50$ Å are negative. Values of 2.39 Å and 2.44 Å were evidenced between $Fe(j_1)$–$Fe(k_2)$ and $Fe(j_1)$–$Fe(j_1)$ atoms, respectively in $Nd_2Fe_{14}B$ compound. A similar situation was shown in R_2Fe_{17} compounds, where the distances between Fe(f)–Fe(f), Fe(g)–Fe(k), Fe(g)–Fe(j) and Fe(k)–Fe(k) are smaller than 2.50 Å [4]. The interactions between iron atoms situated at greater distances than 2.50 Å, are positive and stronger than the negative ones and thus the last ones are not satisfied. Consequently a large magnetic energy is stored. This brings about the low ordering temperatures of R_2Fe_{17} and $R_2Fe_{14}B$ compounds.

In this paper we analyse the possibilities to increase the Curie temperatures of the above systems by diminishing or canceling the negative exchange interactions. Thus, the presence of interstitial atoms in the above crystal structures, increase the lattice constants and thus the distances between iron atoms, with beneficiary effect on T_C values. Similar effect can be obtained substituting iron atoms in sites involved in negative exchange interactions. In the following we report the results of band structure calculations performed on $R_2Fe_{14}B$ and R_2Fe_{17} compounds and we analyse the exchange interactions in these systems. Then, we analyse the effect of replacing iron atoms in $Nd_2Fe_{14}B$ compounds by Si as well as by carbonation of R–Fe–Si based alloys.

2. EXPERIMENTAL AND COMPUTING METHOD

The $R_2Fe_{14}B$ samples were prepared by melting the constituent elements in an induction furnace. The samples were thermally treated and analysed by X–ray diffraction. The $Nd_{15}Fe_{77-y}Si_yB_8$ permanent magnets were prepared by melting the constituent elements in an induction furnace. The samples were crushed and milled to 1–2 μm grain sizes. The samples were aligned in magnetic field of 30 kOe and pressed. Then, these were sintered at 1080°C during 1h and thermally treated at temperatures between 580–630°C during 0.5 h. The X–ray analyses show that the magnets are constituted from $Nd_2Fe_{14-x}Si_xB$ and a Nd–rich phases. The last phase surrounds the $Nd_2Fe_{14-x}Si_xB$ hard magnetic grains and reduces dipolar interactions or exchange coupling between misaligned grains.

The Sm–Fe–Si–C system was obtained by high energy ball milling and annealing at 650°C–950°C. The alloys are nanocrystalline with grain sizes of 22–30 nm [5, 6].

Band structure calculations were performed by using the ab initio tight binding linear muffin tin orbital method, in the atomic sphere approximation (TB–LMTO–ASA) [7]. In the framework of the local density approximation (LDA), the total electronic potential is the sum of external, Coulomb and exchange correlation energies [8]. The functional form of the exchange correlation energy, used in the present work, was the free electron gas parameterization of Van–Barth and Hedin [9]. Relativistic effects were included. The 4f states were treated as part of the band structure, but the polarization of the 4f densities was calculated self-consequently.

3. BAND STRUCTURES

The computed iron moments in $R_2Fe_{14}B$ compounds as function of De Gennes factor, $G = (g_J - 1)^2 J(J + 1)$, are plotted in Fig. 1. The variation of the iron moments can be described by the relation:

$$M_{Fe} = M_{Fe}(0) + \alpha G. \quad (1)$$

We denoted by $M_{Fe}(0)$ the iron moment in compounds with nonmagnetic R, as La, Lu, as well Y, where $G = 0$.

The above data show that a fraction of iron moments is induced by 4f–5d–3d exchange interactions. This fraction is of the order 5% from the iron moment.

The R5d band polarizations, M_{5d}, as function of G factor are given in Fig. 2. The M_{5d} values increase rather regularly with G and are paralelly oriented to the R4f

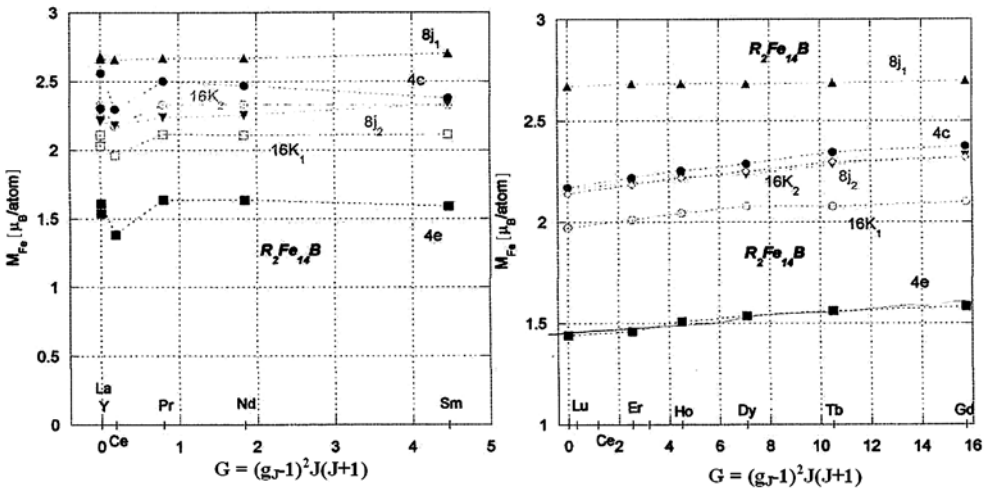

Fig. 1 – The iron magnetic moments in $R_2Fe_{14}B$ compounds as function of de Gennes factor.

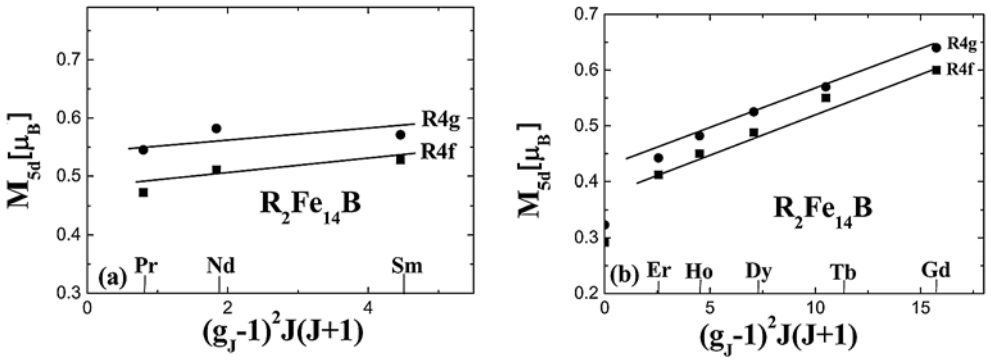

Fig. 2 – The R5d band polarizations in $R_2Fe_{14}B$ compounds.

moments. The $Ce_2Fe_{14}B$ is a peculiar case. In this compound both 4f and 5d states are in band and thus the data obtained include contributions from both bands. The R5d band polarizations are dependent on the lattice sites, although show the same variation, described by:

$$M_{5d} = M_{5d}(0)+\beta G. \tag{2}$$

The above variation suggests the presence of two contributions to the R5d band polarizations. The $M_{5d}(0)$ is due to the 5d–3d short range exchange interactions, and characterizes 5d band polarization of $La_2Fe_{14}B$ or $Lu_2Fe_{14}B$, in which the R element is not magnetic. The βG contributions are due to intra–atomic 4f–5d interactions. The relation (2) can describe exactly the R5d polarizations only if the iron moments are constant along the series. Since there are relatively small

variations of iron moments due to 4f–5d–3d exchange interactions, the $M_{5d}(0)$ values can differ little from one to another compound along the series. This can explain the relative small deviations from the linear behaviour shown in Fig. 2.

The analyses of the results of band structure calculations on R_2Fe_{17} compounds (Figs. 3 and 4) suggest the same type of dependences for iron moments and R5d band polarizations as in $R_2Fe_{14}B$ system. The iron moments follow the relation (1) with $\alpha = 4\cdot10^{-2}\mu_B$, very close to $\alpha = 5\cdot10^{-2}\mu_B$ evidenced in $R_2Fe_{14}B$ compounds with heavy rare-earths. The same β values were obtained in both systems, namely $\beta = 1\cdot10^{-2}\mu_B$.

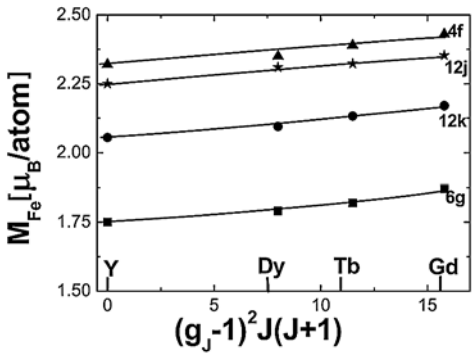

Fig. 3 – The iron moments in R_2Fe_{17} compounds with (R = Gd, Tb, Dy, Y) as function of De Gennes factor.

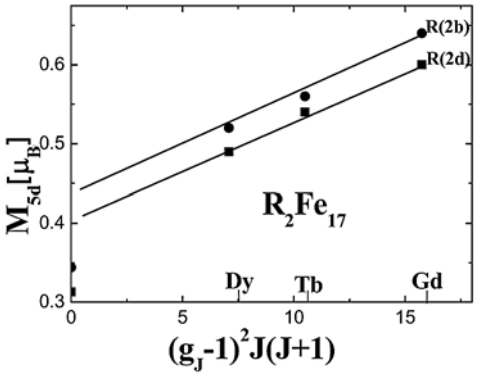

Fig. 4 – The R5d band polarization in R_2Fe_{17} compounds (R = Gd, Tb, Dy, Y).

The differences in the R5d band polarizations at 4f and 4g sites in $R_2Fe_{14}B$ compounds and at 2b and 2d sites in R_2Fe_{17} ones can be correlated with the different strength of 5d–3d exchange interactions, due to their different local environments.

We note that in R_2Fe_{17} compounds, the orbital contribution of iron must be considered in band structure calculations. Thus, when both spin and orbital contributions are taken into account the magnitude of the iron moments follow the sequence $M_{Fe}(f) > M_{Fe}(j) > M_{Fe}(k) > M_{Fe}(g)$. When only spin contribution was taken into account, in the above sequence, $M_{Fe}(f)$ and $M_{Fe}(j)$ are inverted. In both systems the computed mean iron moments are of $2.1–2.2\mu_B$, close to that of pure iron.

As mentioned already, the $M_{5d}(0)$ values were attributed to short range 5d–*n*d ($n = 3, 5$) exchange interactions. These interactions can be described by the Hamiltonian [10]:

$$H = -2J_{5d-3d}S_{5d}(0)\sum_i S_{3d_i}(0) - 2J_{5d-5d}S_{5d}(0)\sum_j S_{5d_j} \qquad (3)$$

We denoted by $J_{3d\text{-}5d}$ and $J_{5d\text{-}5d}$ the exchange parameters characterizing the 3d–5d and 5d–5d interactions with i and j nearest neighbour M an R atoms, respectively.

The relation (3) can be analysed in the molecular field approximation. The effect of 5d–3d and 5d–5d exchange interactions are equivalent to an effective field, $H_{exch,}$ acting on R atom. This induces an additional band polarization $M_{5d}(0)$, to that resulting from intra–atomic 4f–5d exchange. The situation is similar to that evidenced in RM_x compounds where an additional M moment is induced by the internal exchange field. The M magnetic moment was shown, above a critical field, to be linearly dependent on the exchange field [11]. Thus, the induced $M_{5d}(0)$ band polarization can be described by a relation of the form $M_{5d}(0) = \gamma M_d$, where M_d is the total d magnetization [10]. We supposed, in a first approximation that $J_{3d\text{-}5d} \cong J_{5d\text{-}5d}$. The above relation can be shown in R_2M_{17} (M = Fe,Co or Ni) and $R_2Fe_{14}B$ compounds (Fig. 5) where a $\gamma = (2.8 \pm 0.4)\cdot 10^{-2}$ value was determined [12].

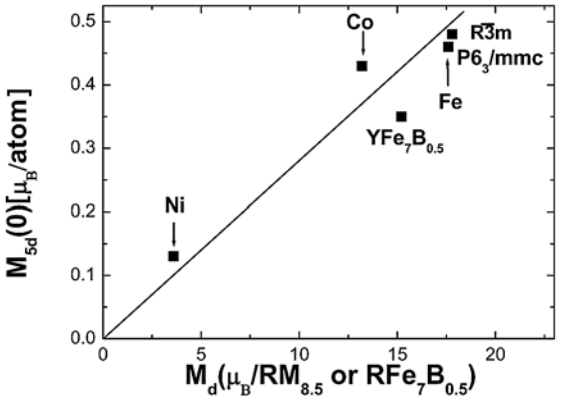

Fig. 5 – The $M_{5d}(0)$ contributions to 5d band polarizations as a function of the total d magnetic moments, M_d, in $RM_{8.5}$ (M = Fe,Co,Ni) compounds as well as the $M_{5d}(0)$ polarization in $Y_2Fe_{14}B$.

Comparing the above value with the induced M moments in RCo_x and RFe_x compounds by the exchange fields, we conclude that the induced 5d band polarizations are of the same order of magnitude as for the cobalt induced moments in RCo_2 compounds [11].

4. Nd-Fe-Si-B PERMANENT MAGNETS

The hard magnetic properties of Nd-Fe-Si-B alloys are mainly determined by the $Nd_2Fe_{14-x}Si_xB$ hard magnetic phase. Previous studies on $Nd_2Fe_{14-x}Si_xB$ showed that the Curie temperatures increase as result of silicon substitution [2]. This behaviour is connected with the Si site occupancy in $Nd_2Fe_{14}B$ lattice, which contribute to the decrease of negative exchange interactions. Thus, in spite of the fact

that Si is nonmagnetic, the above effect surpasses the diminution of positive exchange interactions due to magnetic dilution effects. The anisotropy fields also increase when an iron content, of the order of 0.5 atoms are substituted by Si, Al or Be (Fig. 6).

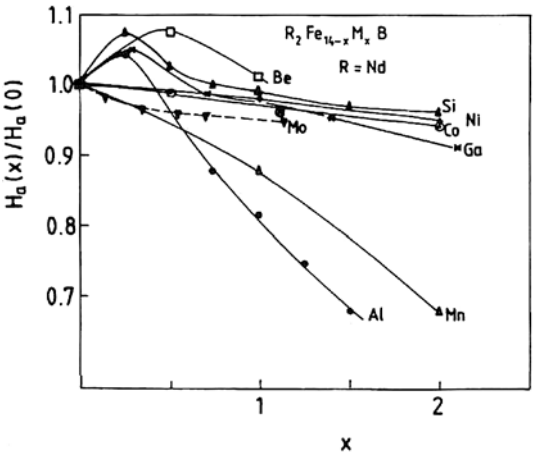

Fig. 6 – Composition dependences of the reduced anisotropy field $H_a(x)/H_a(0)$ for $Nd_2Fe_{14-x}M_xB$ compounds.

Taking the above into account we analysed the magnetic properties of $Nd_{15}Fe_{77-y}Si_yB_8$ alloys with $y \leq 3$. Some demagnetizing curves are shown in Fig. 7, evidencing the influence of composition and thermal treatments on the remanent inductions, B_r and coercive fields, H_c. For the same thermal treatment procedure, there is an increase of the coercive field, as the silicon content varies from $y = 1$ to $y = 2$ (Fig. 8). The composition $Nd_{15}Fe_{75}Si_2B_8$ involves 0.4 iron atoms substituted by

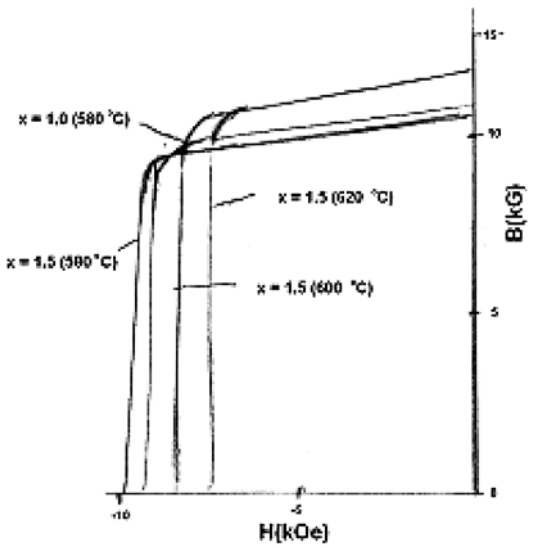

Fig. 7 – Demagnetizing curves for some $Nd_{15}Fe_{77-y}Si_yB_8$ magnets.

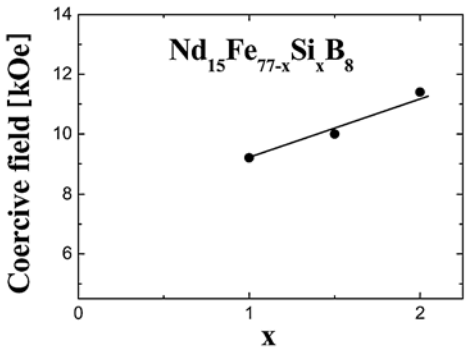

Fig. 8 – Composition dependence of the coercive field in $Nd_{15}Fe_{77-y}Si_yB_8$ magnets.

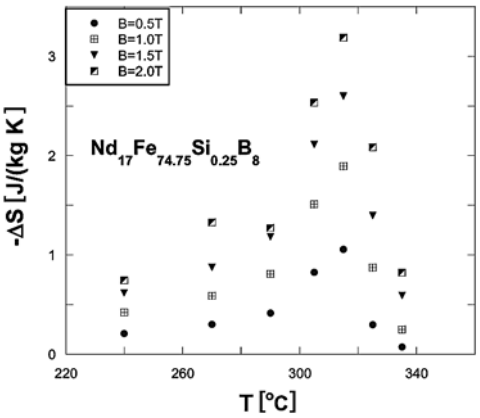

Fig. 9 – The entropy change in $Nd_{15}Fe_{76}Si_1B_8$.

silicon in the hard magnetic phase. For this composition both the increase of the anisotropy field as well as the Curie temperature, contribute to higher coercive field, than for $x = 0$.

The magnetocaloric effect was determined in $Nd_{15}Fe_{77-y}Si_yB$ magnets, starting from magnetization isotherms. The entropy change, ΔS_m, was determined according to the relation [13]

$$\Delta S_m = \sum_i \frac{1}{T_{i+1} - T_i}(M_{i+1} - M_i)_H \Delta H_i, \tag{4}$$

where M_i and M_{i+1} are the magnetizations measured in field H, at temperatures, T_i and T_{i+1}, respectively.

As example, the temperature and field dependences of the magnetic entropy change for $Nd_{15}Fe_{76}SiB_8$ alloys are plotted in Fig. 9. The ΔS_m *vs.* T curves show asymmetric form. The higher absolute value of $|\Delta S_m| = 3.1$ J/kgK was evidenced at a temperature close to the Curie point.

5. Sm-Fe-Si-C ALLOYS

In the R-Fe system no presence of hexagonal $CaCu_5$ type structure was shown. This structure was evidenced in R-Co system, although deviations from 1/5 stoichiometry was shown [1]. The compositions of these compounds can be described by the formula $R_{1-s}Co_{5-2s}$, where s rare-earth atoms were substituted by s dumbbell pairs [14, 15]. The presence of metastable $R_{1-s}Fe_{5+2s}$ phases was also

reported [5, 6]. For $s = 0.22$ a $TbCu_7$ type structure can be invoked, while for $s = 0.36$–0.38, a 1/9 stoichiometry was shown. In this composition range the alloys have a hexagonal P6/mmm type structure. If $s = 0.33$, a single R atom out of three is substituted for by one dumbbell pair and the stoichiometry is 2/17. If the dumbbell pairs are randomly distributed, the structure is hexagonal. The corresponding P6/mmm type structure changes to a rhombohedral $R\bar{3}m$ type though an ordering process of atoms, when the annealing temperature was higher than 850°C.

We showed already that the R_2Fe_{17} compounds although have high saturation magnetizations, the Curie temperatures are rather low since of the presence of unsatisfied negative interactions due short distances between some iron atoms. The lattice parameters can be expanded by introducing the interstitial atoms, as C, in the corresponding lattice. Thus, the negative exchange interactions can be diminished or canceled. For this reason, metastable hexagonal alloys $SmFe_{9-y}Si_yC_z$ as well as $Sm_2Fe_{17-x}Si_xC_u$ were prepared. The C content was $z = 1$ and $u = 2$ [5, 6].

The composition dependences of the Curie temperatures, T_C in both systems before and after carbonation are plotted in Fig. 10 [12]. The T_C values of noncarbonated samples increase gradually when substituting Fe by Si in both systems. The Curie temperatures of the 1/9 phases are higher by ≅ 25 K than those of the 2/17 one. The increase of the Curie temperatures in non-carbonated samples can be attributed to the diminution of antiferromagnetic interactions, due to a slight increase of Fe-Fe distances, consistent with the filling of Fe3d band by Sip electrons, implying a shift to a strong ferromagnetic behaviour.

The Curie temperatures of the carbonated samples are sensitively higher than those of the noncarbonated ones. Due to the increase of lattice parameters, as result of the presence of interstitial carbon, the distances between iron atoms becomes larger

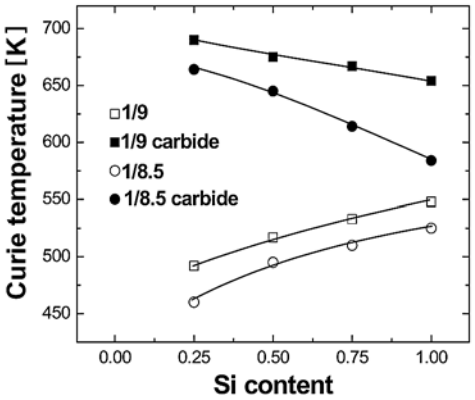

Fig. 10 – Composition dependences of the Curie temperatures in $SmFe_{9-y}Si_yC$ and $SmFe_{8.5-x/2}Si_{x/2}C$ alloys.

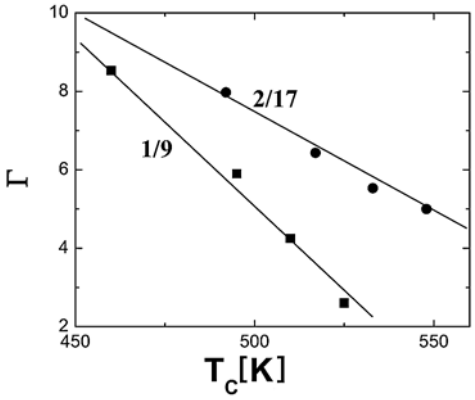

Fig. 11 – The dependence of the Γ values on the Curie temperatures in 1/9 and 2/17 Sm-Fe-Si-C alloys.

than 2.50 Å. As a result, the negative exchange interactions between some iron pairs are near cancelled. When substituting Fe by Si in carbonated samples, a decrease of T_C values is shown, as result of magnetic dilution effects as well as of the hybridization of Fe3d band with Sip and Cp ones.

The correlation between the Curie temperatures and the volume, v, variations can be analysed by using the $\Gamma = d\ln T_C/d\ln v$ parameter [16, 17]. A linear dependence of the Γ values on the Curie temperatures was predicted starting from a model which considers the 3d electrons as having mainly a localized behaviour [16, 18]. In this case the Γ value is described by the relation

$$\Gamma = \frac{5}{3} + 2\frac{d\ln J_{eff}}{d\ln v} + \frac{5}{8}\frac{k_B N_0 g^2 I}{5(S+1)J_{eff}^2 I_b}, \tag{5}$$

where N in the Avogadro number, g is the Landi factor, I is the effective intra-atomic exchange integral, which is reduced from its bare value, I_b and J_{eff} is the effective exchange coupling parameter. Linear Γ *vs* T_C dependences are found in 1/9 and 2/17 carbonated phases (Fig. 11). These can be described by $\Gamma = a - b\cdot T_C$ relation with $a = 34.5$ and $b = 0.054$ K^{-1} for 2/17 compounds and $a = 47.5$ and $b = 0.085$ K^{-1} for 1/9 alloys. The $\gamma = \dfrac{d\ln J_{eff}}{d\ln v}$ values are 16.4 and 22.9 for 2/17 and 1/9 systems, respectively. These can be compared with $\gamma = 16$ obtained in $Y_2Fe_{17}C(N)_x$ compounds [18]. The above data suggest that iron atoms show mainly a localized magnetic moment both in the 2/17 and 1/9 systems, in agreement with band structure calculations. Also we conclude that the effective exchange interactions are more sensitive to volume variations in the 1/9 system than in 2/17 one.

As a result of carbonation, both 2/17 and 1/9 systems show uniaxial anisotropy, in addition to higher Curie temperatures. Thus, these systems are of interest for technical applications. High coercitives were obtained in metastable $SmFe_{9-y}Si_yC$ nanocrystalline alloys annealed between 700 and 800°C [6]. The coercive fields decrease when decreasing or increasing the annealing temperature outside the above mentioned temperature range. Coercive field of $H_C = 13$ kOe was obtained in case of sample having $y = 0.50$ and grain sizes around 22 nm or 15 kOe in nanocrystalline $SmFe_{8.75}Si_{0.25}C$ alloys. The high coercitives of mechanically alloyed and carbonated samples originate from the presence of 1/9 metastable hexagonal phase.

6. CONCLUSION

The band structure calculations showed that in $R_2Fe_{14}B$ and R_2Fe_{17} type compounds, iron has a rather high degree of localization. The R5d band polarizations

in both systems are due both to 4f-5d intra-atomic exchange as well as to R5d-Fe3d short range exchange interactions. The volume variations of the Curie temperatures in nanocrystalline 1/9 and 2/17 carbonated Sm-Fe-Si alloys have linear T_C dependences, as expected for a system in which iron moment has a rather high degree of localization. The effective exchange interactions in 1/9 phase are more sensitive to volume variations than in case of 2/17 compounds.

The Curie temperatures and coercive fields in $Nd_{15}Fe_{77-y}Si_yB_8$ system increases when iron is substituted by small amount of silicon ($y \leq 2$). High coercitives were evidenced in 1/9 phases of Sm-Fe-Si-C nanocrystalline system.

Acknowledgments. This paper is realized under contract CNCSIS Consortiu Nr.188/15.06.06.

REFERENCES

1. E. Burzo, A. Chelkovski, H. R. Kirchmayr, *Landolt-Börnstein Handbuch*, Springer Verlag, 1990, vol. 19d2.
2. E. Burzo, Rep. Progr. Phys., **61**, 1099 (1998).
3. I.A. Campbell, J. Phys. F: Metal Phys., **2**, L47 (1972).
4. D. Givord, R. Lemaire, IEEE Trans. Magn., **10**, 109 (1979).
5. C. Djega-Mariadassou, L. Bessais, A. Nandra, E. Burzo, Phys. Rev., **B 68** 024406 (2003).
6. L. Bessais, C. Djega-Mariadassou, A. Nandra, M. D. Appay, E. Burzo, Phys Rev., **B69** 064402 (2004).
7. O. K. Anderson, Phys. Rev., **B12**, 5060 (1975); O.K. Anderson, O. Jepsen, Phys. Rev. Letters, **53**, 2571 (1984).
8. R. O. Jones, O. Gunnarson, Rev. Mod. Phys., **61**, 689 (1989).
9. U. von Barth, L. Hedin, J. Phys. C: Solid State Phys., **5**, 1629 (1972).
10. E. Burzo, S.G. Chiuzbaian, M. Neumann, M. Valeanu, L. Chioncel, J. Appl. Phys., **92**, 7362 (2002).
11. E. Burzo, Solid State Commun., **14**, 1295 (1974); J. Less Common Met., **77**, 251 (1981).
12. E. Burzo, C. Djega-Mariadassou in Nanoscale Devices-Fundamental and Applications, Springer Verlag, 2006, pp. 371–385.
13. V. K. Pecharsky, K. A. Gschneidner Jr., J. Appl. Phys., **86**, 565 (1999).
14. K. H. J. Buschow, A. S. Van der Goot, J. Less Common Met., **14**, 323 (1968).
15. D. Givord, J. Laforest, J. Schweizer, F. Tasset, J. Appl. Phys., **50**, 2008 (1978).
16. S. Jaakkola, S. Parviainen, S. Penttila, J. Phys.: Metal Phys., **5**, 543 (1975).
17. M. Brouha, K.H.J. Buschow, J. Appl. Phys., **64**, 1813 (1973).
18. N. Plugaru, M. Valeanu, E. Burzo, IEEE Trans. Magn., **30**, 663 (1994).